The term structure of implied correlations between S&P and VIX markets

Laura Ballotta[a] Ernst Eberlein[b] Grégory Rayée[c]

15th March 2025

Abstract

We develop a joint model for the S&P500 and the VIX indices with the aim of extracting forward looking information on the correlation between the two markets. We achieve this by building the model on time changed Lévy processes, deriving closed analytical expressions for relevant quantities directly from the joint characteristic function, and exploiting the market quotes of options on both indices. We perform a piecewise joint calibration to the option prices to ensure the highest level of precision within the limits of the availability of quotes in the dataset and their liquidity. Using the calibrated parameters, we are able to quantify the leverage effect along the term structure of the VIX options and corresponding VIX futures. We illustrate the model using market data on S&P500 options and both futures and options on the VIX.

Keywords: Lévy processes; time changes; implied correlation; option pricing **2020 Mathematics Subject Classification**: 91G15, 91G20, 91G70, 60E10, 60G51

1 Introduction

Recent years have witnessed the fast development of the market for products related to the VIX index, as they are widely used in risk management strategies and as building blocks for other traded instruments (see Szado (2009) for example). These products are also advocated for the construction of optimally structured portfolios issued by institutional investors (see Bertrand and Prigent (2019) and references therein). A common key ingredient across these applications is the correlation between the S&P and the VIX markets, the quantification of which requires a consistent and tractable model for both indices.

Thus, in this paper we develop a joint model for the S&P500 and the VIX indices with the aim of extracting forward looking information on the term structure of the correlations between the two markets by calibrating to the prices of liquidly traded derivatives such as S&P500 and VIX options, as well as VIX futures. We achieve this by using time changed Lévy processes in the spirit of Carr et al. (2003), Carr and Wu (2004), Huang and Wu (2004) and Ballotta and Rayée (2022), which allows to derive closed analytical expressions for the relevant quantities directly

[a]Corresponding Author: L.Ballotta@citystgeorges.ac.uk, Faculty of Finance, Bayes Business School (formerly Cass), City St George's, University of London, UK

[b]eberlein@stochastik.uni-freiburg.de, Department of Mathematical Stochastics, University of Freiburg, Germany

[c]Head of ALM Analytics, Belfius Banque & Assurances, Brussels, Belgium

from the joint characteristic function. The latter is available thanks to the affine property of the construction. Indeed, the class of affine processes has been restated in terms of time changed Lévy processes by Kallsen (2006). Thus, we base derivatives pricing on Fourier transform techniques (see for example Eberlein et al. (2010)), and data from the CBOE on S&P500 options and both futures and options on the VIX.

The proposed model is built on purely discontinuous processes by means of a suitably designed factor construction inspired by Ballotta and Bonfiglioli (2016), which enables the generation of both stochastic volatility and leverage. The approach is quite flexible concerning the choice of the driving processes, as the only relevant piece of information required is their characteristic function. For the purpose of the empirical analysis, we consider a specification of the proposed setting built on the CGMY process of Carr et al. (2002). Although the construction could be extended to include diffusion components (see Ballotta and Eberlein (2025) for further details), the empirical analysis presented for example by Ballotta and Rayée (2022) highlights their limited added value in terms of calibration performance.

Models based on affine processes have been used in the literature to price options on realized variance and VIX by Sepp (2008a,b), and options on quadratic variation by Kallsen et al. (2011). Our approach differs as the model is based entirely on discontinuous processes, and dependence is induced via a factor construction accommodating both leverage and volatility feedback.

The central contribution of this paper lies in the quantification of the correlation between the (log-returns of the) S&P500 index and the (square of the) VIX index using the market consistent information encapsulated by the VIX index itself and the existing S&P500 and VIX derivatives. The objective is to extract a forward looking term structure for this correlation over the expiry range of traded contracts. The recovery of implied correlation between assets using option prices has been explored in the FX markets by Ballotta et al. (2017), Brigo et al. (2021) and Amici et al. (2025) amongst others; however, to the best of our knowledge, this is the first study involving two different markets, namely the S&P and the VIX markets. We envisage the potential for this term structure of implied correlations to become a relevant market metric, if not even a reference quantity for new derivative products.

Due to the affine construction of the model, we can also gain a forward looking insight into the so-called leverage and volatility feedback effects, whereby leverage indicates the impact on the volatility level of (in general adverse) changes in the log-returns, whilst volatility feedback refers to the decline in equity returns originated by anticipated rises in volatility. In this respect, the VIX market provides the ideal environment to price in such effects. This forward looking approach distinguishes our paper from other contributions in the literature on leverage and volatility feedback which primarily focus on stock and portfolio returns (see for example Carr and Wu (2017) amongst others).

An additional contribution of this paper is a new interpretation of the bias between the VIX index and the conditional mean of the integrated variance. The general specification of the model in fact allows us to identify the origin of this bias in the higher order moments of the Lévy process which is time changed in the dynamics of the S&P500 log-returns. This particular aspect also provides a theoretical ground for the 'fear gauge' nickname the VIX index is usually referred to in the industry: by incorporating information on the skewness and excess kurtosis, the VIX index offers indeed a view on the probability of significant market movements in the 'wrong' direction

(see also the discussion in Ballotta (2024)).

This paper also contributes, albeit indirectly, to the growing literature that explores the joint calibration problem, i.e. the development of models which can simultaneously reproduce the market volatility surfaces of options on the S&P500 and the VIX indices in addition to the prices of VIX futures. Recent works in this direction include Abi Jaber et al. (2023) and Cuchiero et al. (2025) amongst others. Our work, however, differs from these studies in the way in which we manage the variation in the level of the VIX implied volatilities from one maturity to the next during the calibration. Motivated by the observation that a similar variation in scale characterizes the interest rate market as well (although on a significantly different time scale), we adopt a piecewise approach similar to Eberlein and Kluge (2005). In this way we can extract correlation values consistent with the maturities available in the market for the relevant contracts.

The results from the empirical analysis show a significant negative implied correlation between the two markets, indicating a clear diversification potential of VIX instruments, which has important implications for portfolio management decisions.

The paper is organized as follows. In section 2 we develop the model for the log-return process driving the S&P500 index. In section 3 we obtain an useful expression for the VIX index based on its representation via the log-contract, and pricing formulas based on Fourier transform techniques. In section 4 we derive the analytical expression of the correlation. The term structure of the correlation is studied in section 5, in which we perform the joint calibration, and section 6 concludes.

2 The model

The formal definition of the VIX index from the Cboe White Paper Cboe (2023) is

$$\bar{V}(0,\Delta_\tau) = 100 \times \sqrt{\frac{2}{\Delta_\tau} e^{r\Delta_\tau} \sum_i \frac{\Delta K_i}{K_i^2} O(K_i) - \frac{1}{\Delta_\tau}\left(\frac{F_S(0,\Delta_\tau)}{K_0} - 1\right)^2},$$

where r is the risk free interest rate to expiration, $O(K_i)$ is the mid price of out-of-the-money (OTM) call and put options on the S&P500 with strike K_i and time to maturity Δ_τ fixed at 30 days, $F_S(0,\Delta_\tau)$ is the forward index level derived from index option prices, K_0 is the largest available strike below or equal to the forward index level, and ΔK_i is the interval between strikes computed as $(K_{i+1} - K_{i-1})/2$.

For the purpose of pricing derivatives on the VIX, a more convenient expression for the index can be obtained from the price of the log-contract on the S&P500. To this aim, let $(\Omega, \mathcal{F}, \{\mathcal{F}_t\}_{t\geq 0}, \mathbb{P})$ be a filtered probability space, with $\mathbb{P}$ denoting a risk neutral probability measure[1], and denote by $S(t)$ the value of the S&P500 at time t. An application of the static replication formula implies that the VIX can be approximated as $\bar{V}(0,\Delta_\tau) = 100 \times V(0,\Delta_\tau)$, for

$$V(t, t+\Delta_\tau) = \sqrt{-\frac{2}{\Delta_\tau}\mathbb{E}_t\left(\ln \frac{S(t+\Delta_\tau)}{F_S(t,t+\Delta_\tau)}\right)}, \tag{1}$$

[1]We note that the proposed market model is incomplete and consequently the risk neutral martingale measure is not unique. Hence, we follow standard practice for incomplete markets and determine the risk neutral measure through the prices of derivative contracts traded in the market.

with $\mathbb{E}_t(\cdot)$ denoting the conditional expectation under the risk neutral measure. As this equation clarifies the connection to the S&P500 index, in the following we introduce a model for its price process.

2.1 The general specification

We model the equity index price process with spot value $S(0)$ as

$$S(t) = S(0)e^{rt+X(t)},$$

for r the (constant) continuously compounded interest rate, and $X(t)$ a time changed Lévy process.

More in details, let $L(t)$ denote the so-called base process, and $T(t)$ be a stochastic clock, then $X(t) = L(T(t)) = (L \circ T)(t)$. In other words, the process $X(t)$ is obtained by observing the process $L(t)$ on a time scale controlled by $T(t)$. This construction recognizes that price changes are caused by imbalances in demand and supply due to trades. Thus, uncertainty originates from both the timing of the change, which is modelled by the clock $T(t)$ and can be interpreted as business time, and its magnitude which is captured by the base process $L(t)$.

We assume that the base process is defined as

$$L(t) = -\varphi_{J_1}(-\mathrm{i}\sigma_1)t + \sigma_1 J_1(t),$$

for a constant σ_1. In the above equation, $J_1(t)$ is a Lévy process with characteristic exponent $\varphi_{J_1}(u)$ and triplet $(\alpha_1, 0, \nu_1(dx))$, which satisfies the following.

Assumption 1. *There exists a constant $\bar{M}$ such that*

$$\int\limits_{\{|x|>1\}} e^{ux}\nu_1(dx) < \infty \qquad \textit{for all } u \in [-\bar{M}, \bar{M}],$$

i.e. the exponential moments of J_1 are finite.

The above assumption is required to ensure that the price process has finite moments (see for example Eberlein and Kallsen (2019)) and is satisfied by all purely discontinuous processes typically used in mathematical finance such as hyperbolic, Normal Inverse Gaussian, generalized hyperbolic, Variance Gamma and CGMY processes, with the only exception of stable processes.

Assumption 1 implies in particular the finiteness of $\mathbb{E}(J_1(t))$, and consequently $J_1(t)$ can be represented as

$$J_1(t) = \alpha_1 t + \int_0^t \int_{\mathbb{R}} x \left(\mu^{J_1} - \nu^{J_1}\right)(ds, dx),$$

where $\mu^{J_1}(dt, dx)$ is the random measure of the jumps of J_1 with compensator $\nu^{J_1}(dt, dx) = \nu_1(dx)dt$, and $\alpha_1 = \mathbb{E}(J_1(1))$. In other words, Assumption 1 allows us to use the identity function for truncation. Consequently, the characteristic exponent is

$$\varphi_{J_1}(u) = \mathrm{i}u\alpha_1 + \int_{\mathbb{R}} \left(e^{\mathrm{i}ux} - 1 - \mathrm{i}ux\right)\nu_1(dx).$$

For later use, we decompose the process $J_1 = J_{1,-} + J_{1,+}$ into the sum of the (compensated) negative and positive jumps with triplets $(\alpha_{1,-}, 0, \nu_{1,-}(dx))$ and $(\alpha_{1,+}, 0, \nu_{1,+}(dx))$ respectively.

Under the above assumptions, the process $X(t)$ driving the equity index is given by

$$X(t) = -\varphi_{J_1}(-\mathrm{i}\sigma_1)T(t) + \sigma_1 \left(J_1 \circ T\right)(t). \tag{2}$$

For the stochastic clock $T(t)$, we assume that it is absolutely continuous with activity rate $v(t)$, so that

$$T(t) = \int_0^t v(s_-)ds.$$

In particular, we assume that the activity rate as well is originated by a time changed Lévy process of the form

$$v(t) = v(0) + \kappa\theta t + (Y \circ T)(t),$$

for κ and θ positive constants and

$$Y(t) = -\kappa t - \eta_1 J_{1,-}(t) + \eta_2 J_2(t).$$

In other words,

$$v(t) = v(0) + \int_0^t \kappa\left(\theta - v(s_-)\right) ds - \eta_1 \left(J_{1,-} \circ T\right)(t) + \eta_2 \left(J_2 \circ T\right)(t), \tag{3}$$

in which $v(0) > 0$, η_1 and η_2 are non-negative constants, and $J_2(t)$ is a purely discontinuous Lévy process independent of $J_1(t)$, with jumps of positive size, and characteristic exponent $\varphi_{J_2}(u)$. We assume that $J_2(t)$ satisfies Assumption 1 as well, and therefore has characteristic exponent

$$\varphi_{J_2}(u) = \mathrm{i}u\alpha_2 + \int_{\mathbb{R}_+} \left(e^{\mathrm{i}ux} - 1 - \mathrm{i}ux\right) \nu_2(dx).$$

As equation (3) is an implicit equation, we show in section 2.2 that it has a unique non-negative solution.

We note the following points. Time changes are used to equip Lévy processes with stochastic volatility features (see for example Carr et al. (2003), Ballotta and Rayée (2022)). Indeed, the conditional variance of $X(t)$ is proportional to the stochastic clock $T(t)$, and therefore is governed by the dynamics of the activity rate $v(t)$.

Furthermore, in this construction dependence between the log-returns and their variance is induced by a factor construction, inspired by the work of Ballotta and Bonfiglioli (2016), in which the process $(J_{1,-} \circ T)$ can be interpreted as the source of systematic risk, whilst the process $(J_{1,+} \circ T)$ represents the idiosyncratic risk in the dynamics of the log-returns. In this context, the process $(J_{1,-} \circ T)$ could be seen as the transmission channel of the so-called leverage effect meant as increases in the volatility level due to negative return movements. The process $(J_2 \circ T)$ on the other hand could be interpreted as the main driver of the so-called volatility feedback effect.

Finally, we observe on the one hand that discontinuous dynamics of the log-returns increase the model ability to generate a consistent skew slope especially over short maturities as shown for example in Ballotta and Rayée (2022). On the other hand, the factor construction in the design of the volatility process is supported by the study of Jacod and Todorov (2010) amongst others. Hybrid constructions in spirit similar to the one posited in this paper have been used for interest rate modelling by Eberlein and Rudmann (2018).

We also note the following relationships for use in the remaining sections.

$$\begin{aligned}
\mathbb{E}(Y(1)) &= -\kappa - \eta_1\alpha_{1,-} + \eta_2\alpha_2 =: b_1 && (4)\\
\mathbb{E}(L(1)) &= -\varphi_{J_1}(-\mathrm{i}\sigma_1) + \sigma_1\alpha_1 =: b_2 && (5)\\
\mathbb{V}ar(Y(1)) &= \eta_1^2\mathbb{V}ar(J_{1,-}(1)) + \eta_2^2\mathbb{V}ar(J_2(1)) =: \hat{\sigma}_1^2 && (6)\\
\mathbb{V}ar(L(1)) &= \sigma_1^2\mathbb{V}ar(J_1(1)) =: \hat{\sigma}_2^2 && (7)
\end{aligned}$$

and

$$\mathbb{C}ov(L(1), Y(1)) = -\eta_1\sigma_1\mathbb{V}ar(J_{1,-}(1)) =: \hat{\rho}. \quad (8)$$

Finally, it follows from the given construction (see for example Eberlein and Kallsen (2019), Proposition 4.14) that the trivariate process (v, X, T) has differential characteristics $(B, 0, K)$ of the form

$$\begin{aligned}
B &= \begin{pmatrix}\kappa\theta\\0\\0\end{pmatrix} + \begin{pmatrix}b_1\\b_2\\1\end{pmatrix} v_- =: B_0 + B_1 v_- && (9)\\
K(G) &= \left(\int \mathbb{1}_G(-\eta_1 x, \sigma_1 x, 0)\nu_{1,-}(dx) + \int \mathbb{1}_G(0, \sigma_1 z, 0)\nu_{1,+}(dz)\right.\\
&\quad \left. + \int \mathbb{1}_G(\eta_2 y, 0, 0)\nu_2(dy)\right) v_-, && (10)
\end{aligned}$$

for any Borel set G, $0 \notin G$, and therefore it is affine. Consequently, the following holds.

Theorem 1. *The affine system (v, X, T) admits joint conditional characteristic function*

$$\mathbb{E}_s\left(e^{\mathrm{i}wv(t)+\mathrm{i}uX(t)+\mathrm{i}zT(t)}\right) = e^{\Psi_0(w,u,z;t-s)+\Psi_1(w,u,z;t-s)v(s)+\mathrm{i}uX(s)+\mathrm{i}zT(s)}, \quad s < t$$

with the exponents Ψ_0, Ψ_1 solutions to the system of ordinary differential equations

$$\begin{aligned}
\Psi_0'(w,u,z;t-s) &= \kappa\theta\Psi_1(w,u,z;t-s),\\
\Psi_0(w,u,z;0) &= 0\\
\Psi_1'(w,u,z;t-s) &= \mathrm{i}z + \varphi_L(u) - \kappa\Psi_1(w,u,z;t-s) + \varphi_{J_{1,-}}\left(\mathrm{i}\eta_1\Psi_1(w,u,z;t-s) + u\sigma_1\right)\\
&\quad -\varphi_{J_{1,-}}(\sigma_1 u) + \varphi_{J_2}\left(-\mathrm{i}\eta_2\Psi_1(w,u,z;t-s)\right),\\
\Psi_1(w,u,z;0) &= \mathrm{i}w,
\end{aligned}$$

for $\varphi_L(u) = -\mathrm{i}u\varphi_{J_1}(-\mathrm{i}\sigma_1) + \varphi_{J_1}(\sigma_1 u)$.

Proof. As (v, X, T) is affine, we obtain

$$\mathbb{E}_s\left(e^{\mathrm{i}wv(t)+\mathrm{i}uX(t)+\mathrm{i}zT(t)}\right) = e^{\Psi_0(w,u,z;t-s)+\Psi_1(w,u,z;t-s)v(s)+\Psi_2(w,u,z;t-s)X(s)+\Psi_3(w,u,z;t-s)T(s)}.$$

The exponents Ψ_0, $\boldsymbol{\Psi} = (\Psi_1, \Psi_2, \Psi_3)$ satisfy

$$\begin{aligned}
\Psi_0'(w,u,z;t-s) &= \boldsymbol{\Psi} B_0 \\
\Psi_0(w,u,z;0) &= 0, \\
\Psi_1'(w,u,z;t-s) &= \boldsymbol{\Psi} B_1 + \int_{\mathbb{R}} \left(e^{\boldsymbol{\Psi}(-\eta_1 x, \sigma_1 x, 0)^\top} - 1 - \boldsymbol{\Psi}(-\eta_1 x, \sigma_1 x, 0)^\top \right) \nu_{1,-}(dx) \\
&\quad + \int_{\mathbb{R}} \left(e^{\boldsymbol{\Psi}(0, \sigma_1 z, 0)^\top} - 1 - \boldsymbol{\Psi}(0, \sigma_1 z, 0)^\top \right) \nu_{1,+}(dz) \\
&\quad + \int_{\mathbb{R}} \left(e^{\boldsymbol{\Psi}(\eta_2 y, 0, 0)^\top} - 1 - \boldsymbol{\Psi}(\eta_2 y, 0, 0)^\top \right) \nu_2(dy), \\
\Psi_1(w,u,z;0) &= \mathrm{i}w,
\end{aligned}$$

and

$$\begin{aligned}
\Psi_2'(w,u,z;t-s) &= 0, \quad \Psi_2(w,u,z;0) = \mathrm{i}u, \\
\Psi_3'(w,u,z;t-s) &= 0, \quad \Psi_3(w,u,z;0) = \mathrm{i}z.
\end{aligned}$$

The last two sets of equations imply that $\Psi_2(w,u,z;t-s) = \mathrm{i}u$ and $\Psi_3(w,u,z;t-s) = \mathrm{i}z$. Furthermore, by direct calculation

$$\begin{aligned}
\Psi_0'(w,u,z;t-s) &= \kappa\theta \Psi_1(w,u,z;t-s), \\
\Psi_0(w,u,z;0) &= 0,
\end{aligned}$$

and

$$\begin{aligned}
\Psi_1'(w,u,z;t-s) &= \mathrm{i}z - (\kappa + \eta_1 \alpha_{1,-})\, \Psi_1(w,u,z;t-s) - \mathrm{i}u\varphi_{J_1}(-\mathrm{i}\sigma_1) + \mathrm{i}u\sigma_1\alpha_1 + \eta_2\alpha_2 \Psi_1(w,u,z;t-s) \\
&\quad + \int_{\mathbb{R}} \left(e^{-(\Psi_1(w,u,z;t-s)\eta_1 - \mathrm{i}u\sigma_1)x} - 1 + (\Psi_1(w,u,z;t-s)\eta_1 - \mathrm{i}u\sigma_1)\, x \right) \nu_{1,-}(dx) \\
&\quad + \int_{\mathbb{R}} \left(e^{\mathrm{i}u\sigma_1 z} - 1 - \mathrm{i}u\sigma_1 z \right) \nu_{1,+}(dz) \\
&\quad + \int_{\mathbb{R}} \left(e^{\Psi_1(w,u,z;t-s)\eta_2 y} - 1 - \Psi_1(w,u,z;t-s)\eta_2 y \right) \nu_2(dy), \\
\Psi_1(w,u,z;0) &= \mathrm{i}w.
\end{aligned}$$

The result follows from this. □

2.2 Existence and non-negativity of the activity rate process $v(t)$

In order to prove that there is a unique non-negative solution to the implicit equation (3), we represent $v(t)$ as the solution to an affine martingale problem. For this purpose, define the linear maps $g_1 : \mathbb{R}_- \to \mathbb{R}_+$, $g_1(x) = -\eta_1 x$ and $g_2 : \mathbb{R}_+ \to \mathbb{R}_+$, $g_2(x) = \eta_2 x$, and the corresponding measure transformations $g_1(\nu_{1,-})(B) = \nu_{1,-}(g_1^{-1}(B))$ and $g_2(\nu_2)(B) = \nu_2(g_2^{-1}(B))$. Consider $\tilde{J}_{1,-}(t) = -\eta_1 J_{1,-}(t)$ and $\tilde{J}_2(t) = \eta_2 J_2(t)$, then it follows that

$$\begin{aligned}
\varphi_{\tilde{J}_{1,-}}(u) &= -\mathrm{i}u\eta_1\alpha_{1,-} + \int_{\mathbb{R}_+} \left(e^{\mathrm{i}uz} - 1 - \mathrm{i}uz \right) g_1(\nu_{1,-})(dz) \\
\varphi_{\tilde{J}_2}(u) &= \mathrm{i}u\eta_2\alpha_2 + \int_{\mathbb{R}_+} \left(e^{\mathrm{i}uz} - 1 - \mathrm{i}uz \right) g_2(\nu_2)(dz).
\end{aligned}$$

The process $J(t) = \tilde{J}_{1,-}(t) + \tilde{J}_2(t)$ has Lévy measure $\nu_J = g_1(\nu_{1,-}) + g_2(\nu_2)$ and characteristic exponent

$$\varphi_J(u) = \mathrm{i}u\left(\eta_2\alpha_2 - \eta_1\alpha_{1,-}\right) + \int_{\mathbb{R}_+}\left(e^{\mathrm{i}uz} - 1 - \mathrm{i}uz\right)\nu_J(dz).$$

We extract from equations (9) and (10) that the first coordinate of the trivariate process has Lévy-Khintchine triplets $(\kappa\theta, 0, 0)$ and $(b_1, 0, \nu_J)$, leading to the following affine martingale problem

$$\begin{aligned} b(t) &= \kappa\theta + b_1 v(t_-) \\ K(t, dx) &= \nu_J(dx)\, v(t_-). \end{aligned}$$

As $\kappa\theta > 0$ and ν_J is a Lévy measure on the positive half-line which satisfies the required moment condition, according to Proposition 6.5 in Eberlein and Kallsen (2019) (non-negative case), this martingale problem has a unique solution $v(t)$ which is non-negative.

3 The VIX dynamics and derivatives pricing

The analysis in section 2 gives access to a useful expression for the square of $V(t, t+\Delta_\tau)$ (equation (1)) and its characteristic function. The latter provides the basis for the development of efficient pricing routines using Fourier transform techniques, which are instrumental for an efficient calibration of the model to market quotes.

3.1 The VIX squared and its characteristic function

Equation (1) shows the link between the VIX index and the log-contract, which in a diffusion setting leads to the identity between the VIX squared and the variance swap rate. However, as discussed in Carr and Wu (2006), when the driving process is a general semimartingale, the identity with the variance swap rate no longer holds due to a correction term incorporating the effects of the jumps. Indeed, we can show that this correction term represents the higher order moments of the base process $L(t)$.

In virtue of equation (1), we have

$$V(t, t+\Delta_\tau)^2 = -\frac{2}{\Delta_\tau}\mathbb{E}_t\left(\ln\frac{S(t+\Delta_\tau)}{F_S(t, t+\Delta_\tau)}\right).$$

By construction

$$\mathbb{E}_t\left(\ln\frac{S(t+\Delta_\tau)}{F_S(t, t+\Delta_\tau)}\right) = \mathbb{E}_t\left(X(t+\Delta_\tau) - X(t)\right),$$

consequently, we obtain from equation (2)

$$\begin{aligned} \mathbb{E}_t\left(\ln\frac{S(t+\Delta_\tau)}{F_S(t, t+\Delta_\tau)}\right) &= -\varphi_{J_1}(-\mathrm{i}\sigma_1)\,\mathbb{E}_t\left(T(t+\Delta_\tau) - T(t)\right) \\ &\quad + \sigma_1\mathbb{E}_t\left(\left(J_1\circ T\right)(t+\Delta_\tau) - \left(J_1\circ T\right)(t)\right). \end{aligned}$$

As the last conditional expectation in the above equation is equal to

$$\alpha_1\mathbb{E}_t\left(T(t+\Delta_\tau) - T(t)\right)$$

(see Proposition 4.14 in Eberlein and Kallsen (2019)), we finally obtain

$$V(t,t+\Delta_\tau)^2 = -\frac{2b_2}{\Delta_\tau}\mathbb{E}_t\left(T(t+\Delta_\tau)-T(t)\right).$$

We note that by means of the above and equation (5), we can write

$$V(0,\Delta_\tau)^2 = \left(\mathbb{V}ar(L(1)) + \frac{1}{3}\mathcal{C}_3(L(1)) + \frac{1}{12}\mathcal{C}_4(L(1)) + \cdots\right)\frac{\mathbb{E}\left(T(\Delta_\tau)\right)}{\Delta_\tau},$$

with $\mathcal{C}_j(L(1))$ denoting the unit time cumulant of order j of the base process. Therefore, the VIX index $\bar{V}(0,\Delta_\tau) = 100 \times V(0,\Delta_\tau)$ carries information concerning not just the variance of the base process, but also the higher order moments such as the ones controlling the skewness and excess kurtosis of the distribution of the base process. Thus, our model offers an insight into the VIX role as the 'fear gauge': by indirectly capturing information about the probability mass in the tails of the log-return distribution, the VIX index provides a view of the market on the probability of significant movements in the 'wrong' direction.

The conditional expectation of the stochastic clock $T(t)$ can be recovered by differentiation of its (log-)characteristic function, which can be obtained from Theorem 1 by setting $w = u = 0$. To this purpose, let

$$c_j(t-s) = -\mathrm{i}\frac{\partial}{\partial z}\Psi_j(0,0,z;t-s)\Big|_{z=0} \qquad j=0,1,$$

then by standard rule of calculus, it follows that

$$\mathbb{E}_s\left(T(t)\right) = c_0(t-s) + c_1(t-s)v(s) + T(s)$$

with the affine coefficients c_0, c_1 solutions to the system of ordinary differential equations

$$\begin{aligned} c_0'(t-s) &= \kappa\theta c_1(t-s), \\ c_0(0) &= 0 \\ c_1'(t-s) &= 1 + b_1 c_1(t-s), \\ c_1(0) &= 0. \end{aligned}$$

This system can be solved analytically and returns

$$c_0(t-s) = \kappa\theta\frac{e^{b_1(t-s)} - 1 - b_1(t-s)}{b_1^2} \tag{11}$$

$$c_1(t-s) = \frac{e^{b_1(t-s)}-1}{b_1}. \tag{12}$$

Consequently

$$V(t,t+\Delta_\tau)^2 = -\frac{2b_2}{\Delta_\tau}\left(c_0(\Delta_\tau) + c_1(\Delta_\tau)v(t)\right); \tag{13}$$

which implies that the characteristic function $\phi_{V^2}(h;t)$ of $V(t,t+\Delta_\tau)^2$ follows from Theorem 1 by setting $w = -2hb_2c_1(\Delta_\tau)/\Delta_\tau$ and $u = z = 0$. Therefore

$$\phi_{V^2}(h;t) = \mathbb{E}\left(e^{\mathrm{i}hV(t,t+\Delta_\tau)^2}\right) = e^{A(h;\Delta_\tau)+A_0(h;t)+A_1(h;t)v(0)} \tag{14}$$

with

$$A(h;\Delta_\tau) = -\mathrm{i}h\frac{2b_2}{\Delta_\tau}c_0(\Delta_\tau),$$

and the exponents A_0, A_1 solutions to the system

$$\begin{aligned}
A_0'(h;t) &= \kappa\theta A_1(h;t),\\
A_0(h;0) &= 0\\
A_1'(h;t) &= -\kappa A_1(h;t) + \varphi_{J_{1,-}}\left(i\eta_1 A_1(h;t)\right) + \varphi_{J_2}\left(-i\eta_2 A_1(h;t)\right),\\
A_1(h;0) &= -\mathrm{i}h\frac{2b_2}{\Delta_\tau}c_1(\Delta_\tau).
\end{aligned}$$

3.2 The characteristic function of the process $X(t)$

In order to price options on the S&P500 in this setting, we also require the characteristic function of $X(t)$. This follows from Theorem 1 by setting $w = 0$ and $z = 0$, i.e.

$$\phi_X(u;t) = \mathbb{E}\left(e^{\mathrm{i}uX(t)}\right) = e^{D_0(u;t)+D_1(u;t)v(0)}, \tag{15}$$

with the exponents D_0, D_1 solutions to the system of differential equations

$$\begin{aligned}
D_0'(u;t) &= \kappa\theta D_1(u;t),\\
D_0(u;0) &= 0\\
D_1'(u;t) &= \varphi_L(u) - \kappa D_1(u;t) + \varphi_{J_{1,-}}\left(\mathrm{i}\eta_1 D_1(u;t) + \sigma_1 u\right)\\
&\quad - \varphi_{J_{1,-}}\left(\sigma_1 u\right) + \varphi_{J_2}\left(-\mathrm{i}\eta_2 D_1(u;t)\right),\\
D_1(u;0) &= 0.
\end{aligned}$$

Alternatively, the expression for the characteristic function can be obtained adopting the leverage neutral measure approach of Carr and Wu (2004) (see also Ballotta and Rayée (2022)). To this purpose, let us define

$$\gamma(t) = e^{\mathrm{i}uL(t)-\varphi_L(u)t};$$

this process is a martingale starting at 1. Consequently, the time-changed process

$$M(t) = M^u(t) = (\gamma\circ T)(t) = e^{\mathrm{i}uX(t)-\varphi_L(u)T(t)}$$

is a martingale too and defines the density process for a complex-valued 'measure' $\mathbb{M}$ such that

$$\mathbb{E}\left(e^{\mathrm{i}uX(t)}\right) = \mathbb{E}^{\mathbb{M}}\left(e^{\varphi_L(u)T(t)}\right). \tag{16}$$

In other words, the change of measure allows us to operate as if the process of the log-returns were independent of its volatility, i.e. as if there were no leverage (see Carr and Wu (2004)).

3.3 Pricing derivatives: a Fourier based approach

Among the available approaches for option pricing, we adopt the method of Eberlein et al. (2010).

Thus, the prices of call and put options on the S&P500, denoted as $\pi_{SPX}(K,\tau)$, are computed

as

$$\pi_{SPX}(K,\tau) = e^{-r\tau}\frac{e^{-Rs}}{\pi}\int_0^\infty \Re\left(e^{-ius}\phi_X(u-\mathrm{i}R;\tau)\frac{K^{1-R-\mathrm{i}u}}{(1-R-\mathrm{i}u)(-R-\mathrm{i}u)}\right)du,$$

with $R > 1$ for the case of the call option and $R < 0$ for the case of the put option (see Eberlein et al. (2010) for full details on the method), and $s = -\ln F_S(0,\tau)$. The characteristic function $\phi_X(\cdot;\tau)$ is given by equation (15).

For the computation of the price of the VIX call option with payoff

$$C(\bar{V}(\tau,\tau+\Delta_\tau)) = 100\times\left(V(\tau,\tau+\Delta_\tau)-K\right)^+,$$

we proceed as follows. Given the availability of the characteristic function $\phi_{V^2}(\cdot;t)$, we first re-express the payoff as

$$C(\bar{V}(\tau,\tau+\Delta_\tau)) = 100\times\left(\sqrt{V(\tau,\tau+\Delta_\tau)^2}-K\right)^+,$$

and then we derive the Fourier transform $\hat{f}$ of $f(x) = (\sqrt{x}-K)^+$. Thus, for $z\in\mathbb{C}$

$$\begin{aligned}\hat{f}(z) &= \int_{K^2}^\infty e^{\mathrm{i}zx}\left(\sqrt{x}-K\right)dx \\ &= -\frac{1}{\mathrm{i}z}\int_{K^2}^\infty \frac{e^{\mathrm{i}zx}}{2\sqrt{x}}dx\end{aligned}$$

where the last equality holds for $\Im(z) > 0$. This integral can be solved by substitution: set $y = \sqrt{-\mathrm{i}zx}$, then

$$\begin{aligned}\hat{f}(z) &= \frac{1}{(-\mathrm{i}z)^{3/2}}\int_{K\sqrt{-\mathrm{i}z}}^\infty e^{-y^2}dy \\ &= \frac{\sqrt{\pi}}{2(-\mathrm{i}z)^{3/2}}\left(1-\mathrm{erf}(K\sqrt{-\mathrm{i}z})\right),\end{aligned} \tag{17}$$

with $\mathrm{erf}(\cdot)$ denoting the error function of a complex argument. Then, the price of the VIX call option struck at $\bar{K}$ and expiring at τ is given by

$$C_{VIX}(\bar{K},\tau) = 100\times\frac{e^{-r\tau}}{\pi}\int_0^\infty \Re\left(\phi_{V^2}(u-\mathrm{i}R;\tau)\hat{f}(\mathrm{i}R-u)\right)du \tag{18}$$

with r the risk free rate of interest and R the dampening factor. Convergence is ensured for $R > 0$. The relevant characteristic function, $\phi_{V^2}(\cdot;t)$, is given by equation (14). VIX put options can be recovered using the put-call parity, so that

$$C_{VIX}(\bar{K},\tau) - P_{VIX}(\bar{K},\tau) = \mathbb{E}\left(e^{-r\tau}\left(\bar{V}(\tau,\tau+\Delta_\tau)-\bar{K}\right)\right),$$

and therefore

$$P_{VIX}(\bar{K},\tau) = C_{VIX}(\bar{K},\tau) - e^{-r\tau}\left(F_V(0,\tau)-\bar{K}\right). \tag{19}$$

Finally, VIX futures prices are obtained following a procedure similar to Kallsen et al. (2011)

so that

$$\begin{aligned} F_V(0,\tau) &= 100 \times \mathbb{E}(V(\tau, \tau+\Delta_\tau)) \\ &= 100 \times \frac{1}{2\sqrt{\pi}} \int_0^\infty \frac{1-\phi_{V^2}(\mathrm{i}u;\tau)}{u^{3/2}} du \end{aligned}$$

with $\phi_{V^2}(\cdot;t)$ given by equation (14).

The numerical schemes are implemented in `Matlab R2023b`. All integrals are computed by standard quadrature methods fully vectorized for speed, and the relevant differential equations are solved numerically using the Runge-Kutta method. The computation of the error function of a complex argument is carried out by means of the algorithm developed by Godfrey (2024).

4 Second order moments of log-return and activity rate processes

Theorem 1 also gives access to the second order moments and co-moments of the relevant quantities through repeated differentiation. In particular, we focus on the variances of the log-return process $X(t)$ and the activity rate process $v(t)$, and the covariance between them.

In order to define the variance of the process $X(t)$, we use the moments of the base processes defined in equations (4)–(8), and set

$$\begin{aligned} d_0(t) &= \hat{\sigma}_2^2 c_0(t) + 2\hat{\rho}\kappa\theta\frac{b_2}{b_1^2}\left(e^{b_1 t}t + t - 2c_1(t)\right) + \hat{\sigma}_1^2\kappa\theta\frac{b_2^2}{b_1^3}\left(2c_1(t) - 2e^{b_1 t}t - t + \frac{e^{2b_1 t}-1}{2b_1}\right), \\ d_1(t) &= \hat{\sigma}_2^2 c_1(t) + 2\hat{\rho}\frac{b_2}{b_1}\left(e^{b_1 t}t - c_1(t)\right) + \hat{\sigma}_1^2\frac{b_2^2}{b_1^2}\left(\frac{e^{2b_1 t}-1}{b_1} - 2e^{b_1 t}t\right), \end{aligned}$$

with $c_0(t)$ and $c_1(t)$ derived in equations (11)–(12). Then, by repeated differentiation of the joint (log-)characteristic function in Theorem 1, we obtain

$$\mathbb{V}ar(X(t)) = d_0(t) + d_1(t)v(0). \tag{20}$$

Theorem 6.15 in Eberlein and Kallsen (2019) gives access to an alternative derivation of this result. Similarly, set

$$\begin{aligned} q_0(t) &= \kappa\theta\frac{\hat{\sigma}_1^2}{2}c_1^2(t) \\ q_1(t) &= \hat{\sigma}_1^2 e^{b_1 t}c_1(t), \end{aligned}$$

then

$$\mathbb{V}ar(v(t)) = q_0(t) + q_1(t)v(0). \tag{21}$$

Finally,

$$\mathbb{C}ov(X(t), v(t)) = p_0(t) + p_1(t)v(0), \tag{22}$$

for

$$\begin{aligned} p_0(t) &= \kappa\theta\frac{\hat{\rho}}{b_1}\left(e^{b_1 t}t - c_1(t)\right) - \kappa\theta\hat{\sigma}_1^2\frac{b_2}{b_1^2}\left(e^{b_1 t}t - \frac{e^{2b_1 t}-1}{2b_1}\right) \\ p_1(t) &= e^{b_1 t}\left(\hat{\rho}t + \hat{\sigma}_1^2 b_2\frac{c_0(t)}{\kappa\theta}\right). \end{aligned}$$

Figure 1: Correlation between $X(t)$ and $v(t)$: sensitivity analysis with respect to the 'loading' coefficients σ_1, η_1 and η_2. Correlation calculated using equations (20)–(22) for a specific choice of the remaining parameters.

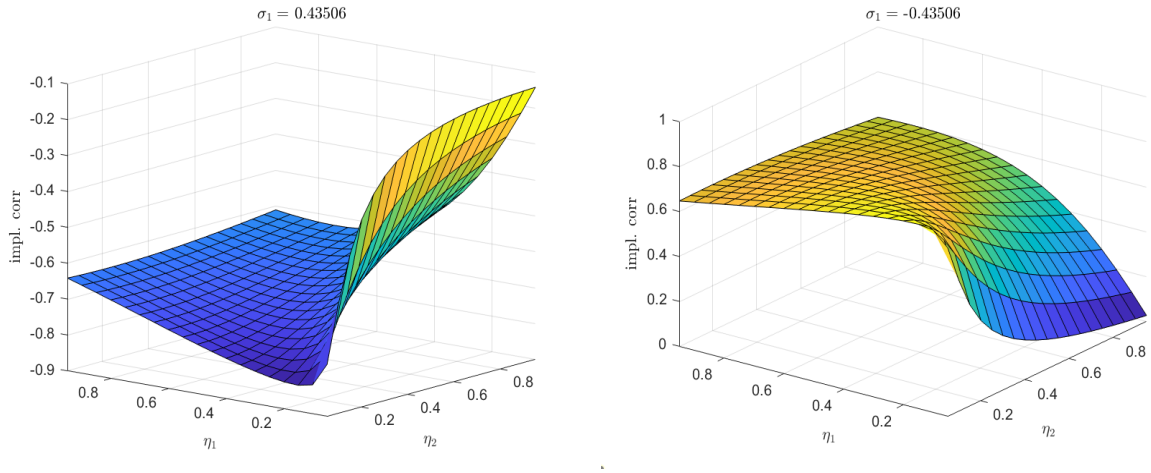

A sketch of the proof is offered in Appendix A for the case of the covariance. The other quantities can be obtained along the same lines.

The expression for the correlation between the log-return process $X(t)$ and the activity rate process $v(t)$ follows directly. In virtue of equation (13), this is the same as the correlation between the S&P500 index log-returns and the VIX squared.

In order to demonstrate the flexibility of the approach, we show in Figure 1 (parameters available upon request) how the correlation changes for different values of the parameters σ_1, η_1 and η_2, which control respectively the level of the correlation between the base processes of the log-returns and the activity rate (see equation (8)), and the impact on the log-returns of the idiosyncratic movements in the activity rate (see equations (2)–(3)).

5 The term structure of implied correlations

In this section we first calibrate this model jointly to market data for options on the S&P500 and the VIX together with VIX futures. We then use the calibrated parameters to extract the term structure of implied correlations by applying the results obtained in section 4.

End of day market prices were collected from the CBOE on May 3rd 2023 for call and put options on both the S&P500 and the VIX indices, together with VIX futures prices. We use mid option prices obtained from the quoted bid and ask prices of out of the money (OTM) contracts.

We apply the commonly adopted exclusion filters to the set of option prices, so that only contracts with positive open interest, bid price and bid-ask spread are selected. Furthermore, we only consider maturity slices with more than 5 traded strikes. For the observation date under consideration, this implies that we can use options on the VIX up to 77 days to expiry as the bulk of liquidity is concentrated around short maturity contracts. The corresponding market implied volatilities are shown in the top panels of Figure 2. The VIX futures prices for the corresponding maturities are shown in the bottom panel of Figure 2 together with the VIX spot value. The term structure of interest rates is extracted from the USD SOFR curve on May 3rd 2023.

Figure 2: A sample of market data. Top-panels: implied volatilities from the S&P500 market (left-hand side panel), and the VIX market (right-hand side panel). Bottom panel: VIX futures prices for maturities corresponding to the ones of VIX options. Source: CBOE. Observation date: May 3^{rd} 2023.

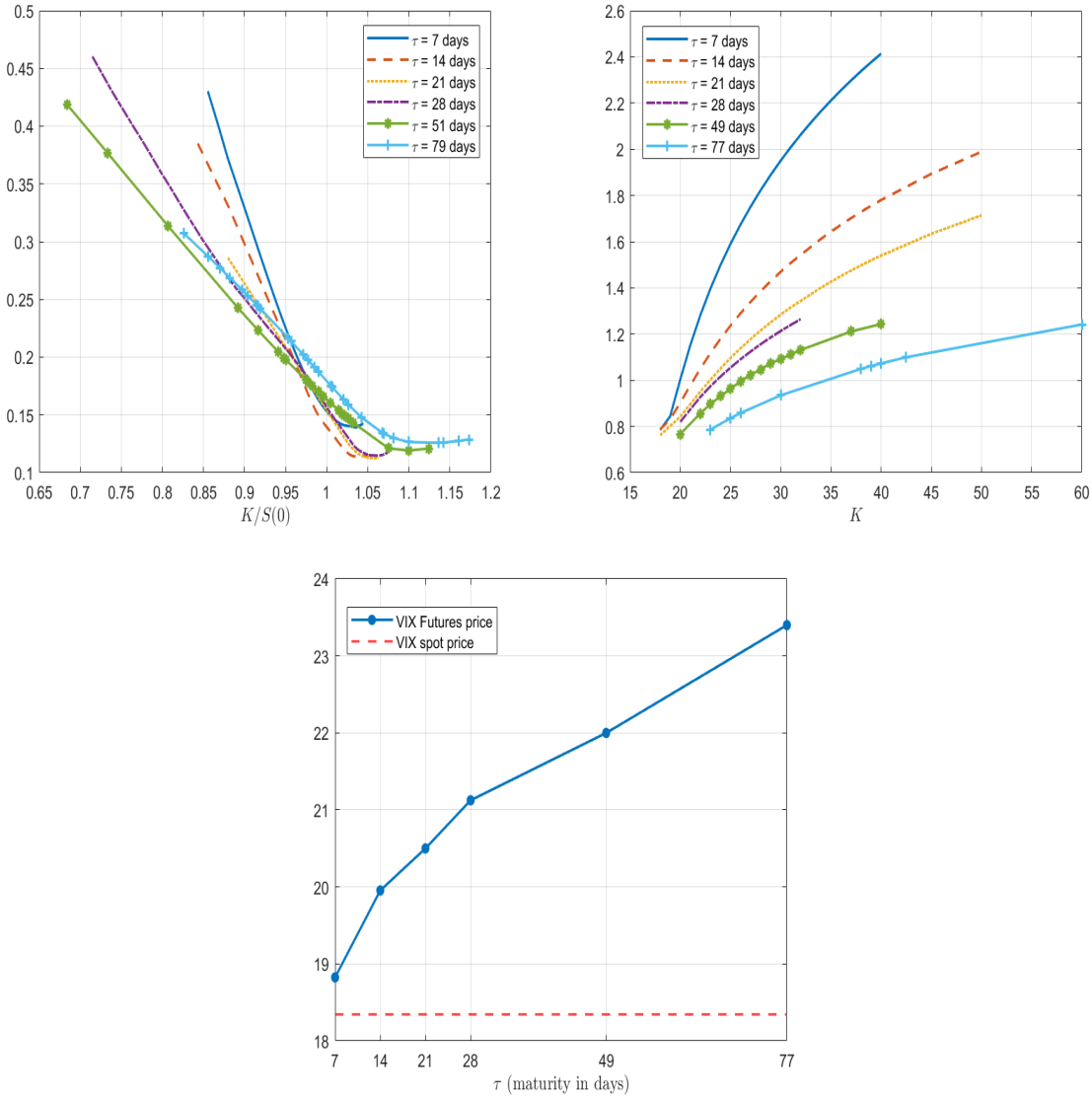

5.1 The joint objective function and the calibration problem

In order to obtain a reliable estimation of the implied correlation, we need to ensure that the model is able to reproduce the market quotes of derivatives as closely as possible. However, from Figure 2 we note two important features of the implied volatilities in the VIX market which can represent a challenge for the calibration procedure. In first place, there is a clear difference in the scale of the implied volatilities between the two markets. Indeed, the level of the VIX implied volatilities is significantly higher than the one of the implied volatilities in the S&P market. Secondly, the level of the VIX implied volatilities varies substantially from one maturity to the next, especially between the first two available maturities, i.e. 7 and 14 days to expiry.

Furthermore, we note that the correct calibration of VIX futures is necessary in order to recover consistent VIX implied volatilities by inversion of the Black formula (see Black (1976)). The inclusion of the futures prices though exacerbates the issue of scale noted above. Therefore, it is crucial to define an appropriate objective function in which all the relevant quantities are

suitably rescaled to ensure comparability.

To this purpose, let

$$f_i(j;\vartheta) = \left(\frac{\pi_i^{mod}(j;\vartheta) - \pi_i^{eod}(j)}{\mathrm{Vol}_i^{eod}(j) Vega_i(j)} \right)^2, \quad i = 1, 2,\ j = 1, \ldots, N_i,$$

where $\pi_i^{eod}(j)$ is the end of day mid market price given by the j-th data point representing either an OTM call or an OTM put option struck at K_j and with maturity τ_j, written on the S&P500 for $i = 1$ and the VIX for $i = 2$ respectively. $\pi_i^{mod}(j;\vartheta)$ denotes the corresponding price originated by the model with parameter set ϑ. In this context, $Vega_i(j)$ denotes the (Black) Vega computed using the market implied volatilities $\mathrm{Vol}_i^{eod}(j)$. N_i is the number of option contracts in the data set.

The ratio between the error of the model price with respect to the market price and the Vega is used as a first order approximation of the implied volatility error; this approximation is chosen to both speed up the calibration and avoid potential bias due to expensive contracts (see for example Christoffersen et al. (2009), Ballotta and Rayée (2022), and references therein). The normalization via the implied volatility guarantees comparability between the two markets, given the observed different ranges of implied volatility values for S&P500 and VIX options.

Furthermore, let

$$f(l;\vartheta) = \left(\frac{\pi^{mod}(l;\vartheta) - \pi^{eod}(l)}{\pi^{eod}(l)} \right)^2,$$

with $\pi^{mod}(l;\vartheta)$ denoting the price of the VIX futures with maturity τ_l for $l = 1, \ldots, N_F$ under the given model, and $\pi^{eod}(l)$ denoting the corresponding end of day market prices. N_F is the number of VIX futures contracts considered. We use relative errors for the prices of the VIX futures to ensure consistency with the option error functions.

Then, the objective function of the joint calibration problem is given by

$$F(\vartheta) = \sum_{i=1}^{2} \frac{1}{N_i} \sum_{j=1}^{N_i} f_i(j;\vartheta) + \frac{1}{N_F} \sum_{l=1}^{N_F} f(l;\vartheta).$$

The rescaling based on the number of contracts accounts for the different sizes of the respective markets, which could otherwise compromise the fit.

The calibration problem is stated as

$$\min_{\vartheta} F(\vartheta),$$

with ϑ within the parameter limits of the chosen model.

It remains to address the issue of the variation in the VIX implied volatility level across maturities. Motivated by the similarity with the interest rate markets, we adopt a piecewise calibration approach similar in spirit to Eberlein and Kluge (2005). To this purpose, we calibrate separately each maturity interval $[\tau_j^{VIX}, \tau_j^{VIX} + \Delta_\tau]$, for $\tau_j^{VIX} \in \{7, 14, 21, 28, 49, 77\}$, i.e. the maturities of VIX options considered here. For options on the S&P500, we refer to contracts with maturities τ_j^{SPX} coincident with τ_j^{VIX} up to two days, according to availability. Consequently, N_1 denotes the number of options on the S&P500 for all strikes available for maturities τ_j^{SPX} and $\tau_j^{VIX} + \Delta_\tau$, whilst N_2 indicates the number of VIX option contracts for all strikes available for

maturity τ_j^{VIX}. The choice to focus on these 'triangles' is motivated by the fact that the VIX by construction encodes information on the forward density of the S&P500 log-returns and their variance (see, for example Yuan (2022), and references therein).

We note that equation (13) for $t = 0$ links directly the initial level of the volatility activity rate $v(0)$ to the square of the spot value of the VIX index. This allows us to ensure that the model matches exactly the current value of the VIX index. Anchoring the calibration procedure to the current state of the VIX market also contributes to speeding up the convergence of the optimization routine.

In the empirical analysis, we assume that the process $J_1(t)$ is the CGMY process of Carr et al. (2003) with Lévy density

$$C\left(\frac{e^{-G|x|}}{|x|^{1+Y}}1_{x<0} + \frac{e^{-Mx}}{x^{1+Y}}1_{x>0}\right),$$

and parameters $C, G, M > 0$, $Y < 2$. The corresponding characteristic exponent is

$$\varphi_{J_1}(u) = C\Gamma(-Y)\left((M - \mathrm{i}u)^Y - M^Y + (G + \mathrm{i}u)^Y - G^Y\right).$$

Finally, we assume that the process $J_2(t)$ is a Gamma process with characteristic exponent

$$\varphi_{J_2}(u) = \beta\left(\ln\lambda - \ln(\lambda - \mathrm{i}u)\right),$$

for $\beta, \lambda > 0$.

5.2 Results

In this section we gauge the performance of the piecewise joint calibration and extract the term structure of implied correlations between the S&P and VIX markets.

Consistently with the definition of the calibration objective function $F(\vartheta)$, we measure the model performance using relative errors based on the implied volatility recovered from the calibrated parameters. Let $\mathrm{Vol}_i^{mod}(j;\vartheta)$ denote this value for the j-th data point, and define

$$\begin{aligned} e_i &= \sum_{j=1}^{N_i}\left(\frac{\mathrm{Vol}_i^{mod}(j;\vartheta) - \mathrm{Vol}_i^{eod}(j)}{\mathrm{Vol}_i^{eod}(j)}\right)^2, \quad i = 1,2, \\ e_F &= \sum_{l=1}^{N_F} f(l;\vartheta). \end{aligned}$$

We measure the pricing performance separately on each market with

$$\epsilon_i = \sqrt{\frac{1}{N_i}e_i}, \quad i = 1,2, \tag{23}$$

$$\epsilon_F = \sqrt{\frac{1}{N_F}e_F}, \tag{24}$$

and on aggregate with

$$\epsilon = \sqrt{\frac{1}{N}\left(e_1 + e_2 + e_F\right)}, \tag{25}$$

for $N = N_1 + N_2 + N_F$.

Table 1: Joint calibration with piecewise approach. Performance measures as defined in eqs. (23)–(25).

Maturity interval	[7, 37]	[14, 44]	[21, 51]	[28, 58]	[49, 79]	[77, 107]
ϵ_1	5.90%	2.54%	3.65%	3.61%	4.07%	2.64%
ϵ_2	2.07%	1.09%	2.49%	1.43%	2.57%	2.95%
ϵ_F	6.65E-03	1.48E-04	1.71E-03	1.43E-03	0.35%	3.93E-03
ϵ	5.42%	2.30%	3.43%	3.39%	3.76%	2.66%

We compare the implied volatilities generated by the model to the market ones for the dataset under consideration in Figure 3, whilst the corresponding performance measures are reported in Table 1 (the calibrated parameters are available upon request). The accuracy of the calibration is comparable across each maturity interval, but it deteriorates in correspondence of those expiries characterised by relatively low liquidity.

The term structure of the implied correlations is obtained along the range of maturities of the VIX futures and VIX options; we then interpolate/extrapolate for each day between the given maturities using a piecewise cubic Hermite interpolating polynomial. The result is shown in Figure 4. The correlation between the log-returns of the S&P500 and the (square) of the VIX index is significantly negative across the considered time horizon, and it justifies the fact that the VIX calls are the contracts more heavily traded as they are perceived as 'disaster insurance'. The hump shape of the curve could be linked to the low liquidity level of the contracts with 28 days to maturity. The result also indicates that the VIX index and its derivatives have a high diversification potential, and it supports the recommendations from Bertrand and Prigent (2019) to include exposures to VIX instruments for the optimal management of structured portfolios.

Finally, as in virtue of equation (13), the implied correlation between the S&P500 log-returns and the VIX squared coincides with the one between the index log-returns and the activity rate $v(t)$, i.e. the process of the 'point-in-time' variance, we can gain forward looking information on the strength of the leverage/volatility feedback effect in the case in which the volatility is priced in directly through the VIX market.

6 Conclusions

We have developed a joint model for the S&P500 and the VIX based on time changed Lévy processes for the valuation of derivatives written on these indices, and ultimately the quantification of the forward looking implied correlation between the two markets. Due to the affine construction of the model, this implied correlation also quantifies the leverage and volatility feedback effects. We stress that, as the parameters are extracted from a joint calibration of derivatives quotes, the obtained result is forward looking in nature.

The investigation based on market quotes shows that the implied correlation is significantly negative over the horizon of the traded maturities considered in this paper, indicating the level of diversification that the VIX and its derivatives can have. This is particularly relevant for portfolio management decisions.

Figure 3: Joint calibration with piecewise approach. Left-hand-side panel: implied volatility of S&P500 options expiring at $\tau_j^{SPX} = \tau_j^{VIX}$ (up to 2 days). Centre panel: VIX futures price (vertical line) and implied volatility of VIX options expiring at τ_j^{VIX}. Right-hand-side panel: implied volatility of S&P500 options expiring at $\tau_j^{VIX} + \Delta_\tau$.

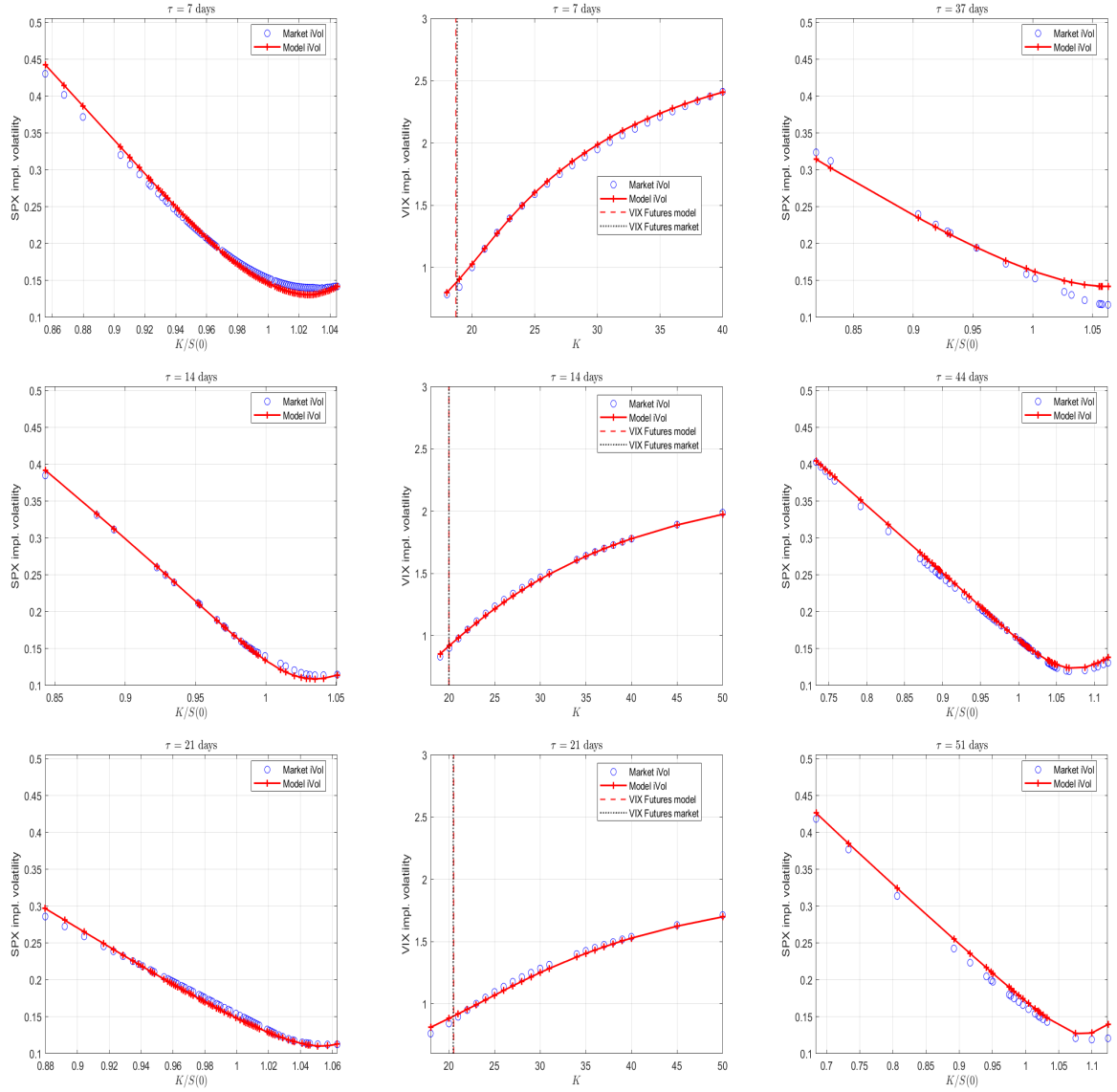

Acknowledgements

An earlier version of this work has been presented at the Quant Summit Europe 2023 in London, the 2024 Bachelier Colloquium in Métabief, the ICCF24 in Amsterdam, the 7th Women in Quantitative Finance Conference 2024 in London, the 12th World Congress of the Bachelier Finance Society 2024 in Rio de Janeiro, and the annual Quant Insights Conference 2024. The paper in its current version has been presented at the Peter Carr Conference on Mathematical Finance at the University of Maryland, QuantMinds International 2024 in London, the FAMiLLY Workshop at the University of York, the Mandelbrot Centennial Colloquium in Paris, and the London-Oxford-Warwick Mathematical Finance Workshop at the University of Oxford. We are grateful to the participants for their useful comments and suggestions. The views expressed in this paper do not necessarily represent those of Belfius Bank. Usual caveat applies.

Figure 3: (cont.) Joint calibration with piecewise approach. Left-hand-side panel: implied volatility of S&P500 options expiring at $\tau_j^{SPX} = \tau_j^{VIX}$ (up to 2 days). Centre panel: VIX futures price (vertical line) and implied volatility of VIX options expiring at τ_j^{VIX}. Right-hand-side panel: implied volatility of S&P500 options expiring at $\tau_j^{VIX} + \Delta_\tau$.

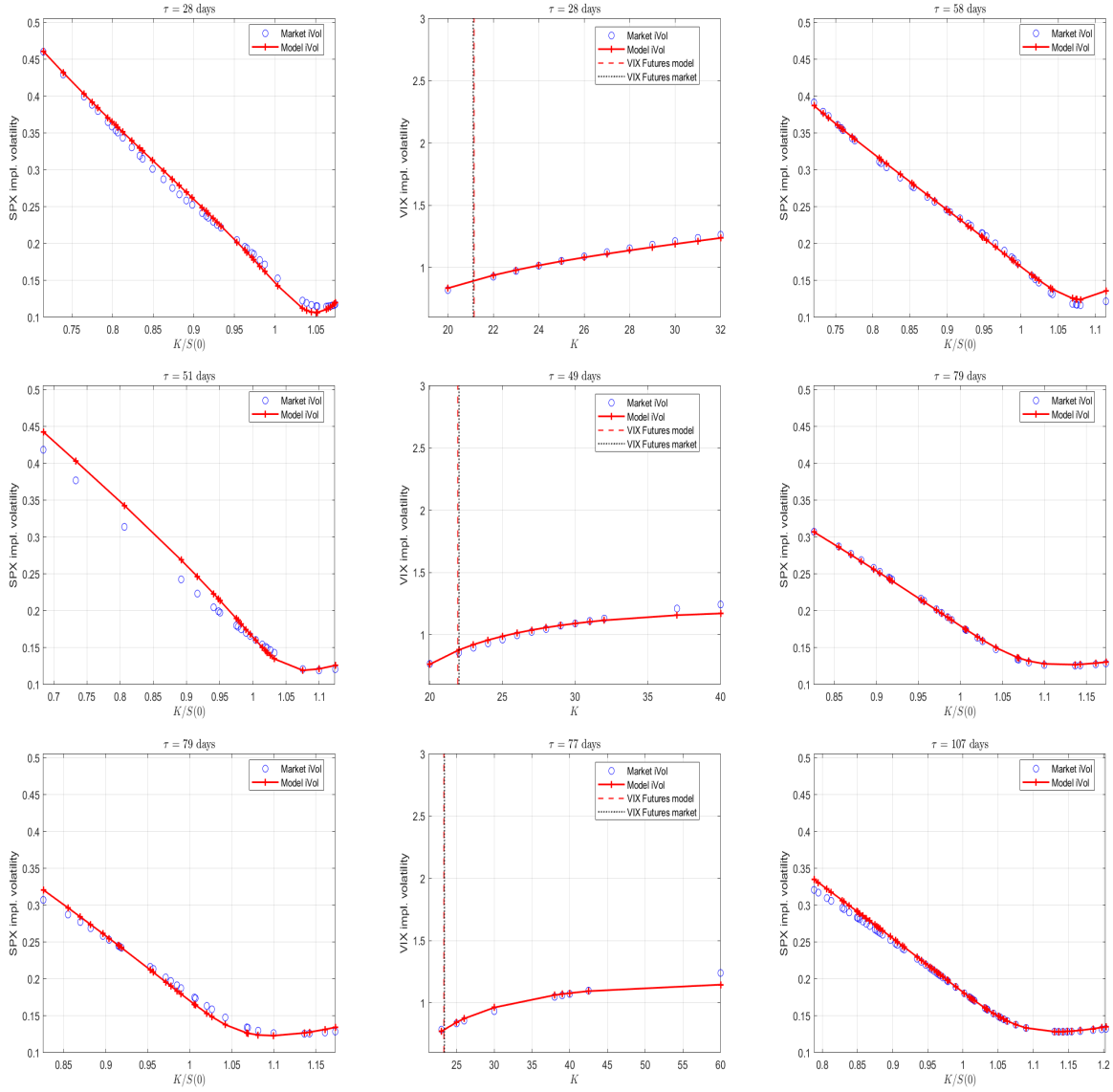

Figure 4: Term structure of implied correlations $\mathbb{C}orr(X(\tau), v(\tau)) = \mathbb{C}orr(X(\tau), V(\tau, \tau + \Delta_\tau)^2)$ obtained from equations (20)-(22) and the calibrated parameters.

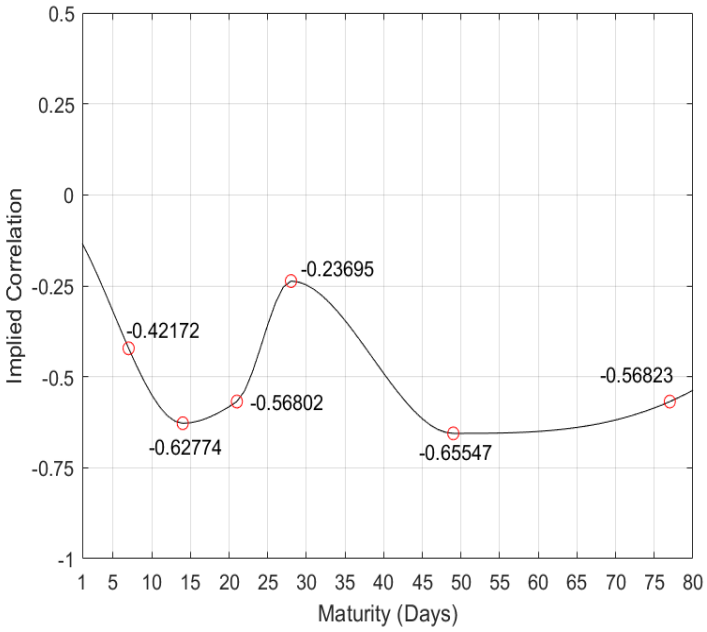

References

Abi Jaber, E., Illand, C., Li, S., 2023. The quintic Ornstein-Uhlenbeck model for joint SPX and VIX calibration. Risk, July, 1–6.

Amici, G., Ballotta, L., Semeraro, P., 2025. Multivariate additive subordination with applications in finance. European Journal of Operational Research 321, 1004–1020.

Ballotta, L., 2024. Is the VIX just volatility? The Devil is in the (de)tails. Wilmott 2024, 18–20.

Ballotta, L., Bonfiglioli, E., 2016. Multivariate asset models using Lévy processes and applications. The European Journal of Finance 22, 1320–1350.

Ballotta, L., Deelstra, G., Rayée, G., 2017. Multivariate FX models with jumps: triangles, quantos and implied correlation. European Journal of Operational Research 260, 1181–1199.

Ballotta, L., Eberlein, E., 2025. Time changes and the leverage neutral measure. Preprint.

Ballotta, L., Rayée, G., 2022. Smiles & smirks: Volatility and leverage by jumps. European Journal of Operational Research 298, 1145–1161.

Bertrand, P., Prigent, J., 2019. On the optimality of path-dependent structured funds: The cost of standardization. European Journal of Operational Research 277, 333–350.

Black, F., 1976. The pricing of commodity contracts. Journal of Financial Economics 3, 167–179.

Brigo, D., Pisani, C., Rapisarda, F., 2021. The multivariate mixture dynamics model: shifted dynamics and correlation skew. Annals of Operations Research 299, 1411–1435.

Carr, P., Geman, H., Madan, D.B., Yor, M., 2002. The fine structure of asset returns: An empirical investigation. Journal of Business 75, 305–332.

Carr, P., Geman, H., Madan, D.B., Yor, M., 2003. Stochastic volatility for Lévy processes. Mathematical Finance 13, 345–382.

Carr, P., Wu, L., 2004. Time-changed Lévy processes and option pricing. Journal of Financial Economics 71, 113–141.

Carr, P., Wu, L., 2006. A tale of two indices. The Journal of Derivatives 13, 13–29.

Carr, P., Wu, L., 2017. Leverage effect, volatility feedback, and self-exciting market disruptions. Journal of Financial and Quantitative Analysis 52, 2119–2156.

Cboe, 2023. Cboe VIX volatility index methodology: Cboe volatility index. Cboe White Paper. Last retrieved: August 2023.

Christoffersen, P., Heston, S., Jacobs, K., 2009. The shape and term structure of the index option smirk: Why multifactor stochastic volatility models work so well. Management Science 55, 1914–1932.

Cuchiero, C., Gazzani, G., Möller, J., Svaluto-Ferro, S., 2025. Joint calibration to SPX and VIX options with signature-based models. Mathematical Finance 35, 161–213.

Eberlein, E., Glau, K., Papapantoleon, A., 2010. Analysis of Fourier transform valuation formulas and applications. Applied Mathematical Finance 17, 211–240.

Eberlein, E., Kallsen, J., 2019. Mathematical Finance. Springer.

Eberlein, E., Kluge, W., 2005. Exact pricing formulae for caps and swaptions in a Lévy term structure model. The Journal of Computational Finance 9, 99–125.

Eberlein, E., Rudmann, M., 2018. Hybrid Lévy models: Design and computational aspects. Applied Mathematical Finance 25, 533–556.

Godfrey, P., 2024. erfz (https://www.mathworks.com/matlabcentral/fileexchange/3574-erfz). MATLAB Central File Exchange. Retrieved July 2024.

Huang, J.Z., Wu, L., 2004. Specification analysis of option pricing models based on time-changed Lévy processes. Journal of Finance 59, 1405–1439.

Jacod, J., Todorov, V., 2010. Do price and volatility jump together? The Annals of Applied Probability 20, 1425–1469.

Kallsen, J., 2006. A didactic note on affine stochastic volatility models, in: Kabanov, Y., Liptser, R., Stoyanov, J. (Eds.), From Stochastic Calculus to Mathematical Finance. The Shiryaev Festschrift. Springer, pp. 343–368.

Kallsen, J., Muhle-Karbe, J., Voß, M., 2011. Pricing options on variance in affine stochastic volatility models. Mathematical Finance 21, 627–641.

Sepp, A., 2008a. Pricing options on realized variance in the Heston model with jumps in returns and volatility. The Journal of Computational Finance 11, 33–70.

Sepp, A., 2008b. VIX option pricing in a jump-diffusion model. Risk, April, 84–89.

Szado, E., 2009. VIX futures and options: A case study of portfolio diversification during the 2008 financial crisis. The Journal of Alternative Investments 12, 68–85.

Yuan, P., 2022. Time-varying skew in VIX derivatives pricing. Management Science 68, 7761–7791.

A Proof of Equation (22)

We note that

$$\mathbb{C}ov(X(t), v(t)) = -\frac{\partial^2}{\partial u \partial w} \ln \mathbb{E}\left(e^{\mathrm{i}wv(t)+\mathrm{i}uX(t)}\right)\Big|_{w=u=0},$$

with the relevant joint characteristic function given by Theorem 1 for $z = 0$. In the following we write for short $\Psi_j(w, u; t) = \Psi_j(w, u, 0; t)$ for $j = 0, 1$; further, we set for $j = 0, 1$

$$\begin{aligned}
\tilde{\Psi}_j(w, u; t) &= \frac{\partial}{\partial u}\Psi_j(w, u; t) \\
\hat{\Psi}_j(w, u; t) &= \frac{\partial}{\partial w}\Psi_j(w, u; t) \\
\bar{\Psi}_j(w, u; t) &= \frac{\partial^2}{\partial u \partial w}\Psi_j(w, u; t).
\end{aligned}$$

We denote $x = \mathrm{i}\eta_1\Psi_1(w, u; t) + u\sigma_1$ and $y = -\mathrm{i}\eta_2\Psi_1(w, u; t)$, and we write the characteristic exponents $\varphi_{J_{1,-}}(\bar{u})$ and $\varphi_{J_2}(\bar{u})$ as functions of the argument $\bar{u}$.

By differentiation with respect to u of the system of ODEs in Theorem 1, we obtain that $\tilde{\Psi}_0(w, u; t)$ and $\tilde{\Psi}_1(w, u; t)$ satisfy the following system of ODEs

$$\begin{aligned}
\tilde{\Psi}_0'(w, u; t) &= \kappa\theta\tilde{\Psi}_1(w, u; t) && \text{(A.1)} \\
\tilde{\Psi}_0(w, u; 0) &= 0 && \text{(A.2)} \\
\tilde{\Psi}_1'(w, u; t) &= \frac{d}{du}\varphi_L(u) + \left(-\kappa + \mathrm{i}\eta_1\frac{d}{d\bar{u}}\varphi_{J_{1,-}}(x) - \mathrm{i}\eta_2\frac{d}{d\bar{u}}\varphi_{J_2}(y)\right)\tilde{\Psi}_1(w, u; t) \\
&\quad + \sigma_1\frac{d}{d\bar{u}}\varphi_{J_{1,-}}(x) - \sigma_1\frac{d}{d\bar{u}}\varphi_{J_{1,-}}(u\sigma_1) && \text{(A.3)} \\
\tilde{\Psi}_1(w, u; 0) &= 0. && \text{(A.4)}
\end{aligned}$$

These ODEs can be used to recover the expected value of $X(t)$ by setting $u = w = 0$ and $h_j(t) = -\mathrm{i}\tilde{\Psi}_j(0, 0; t)$, for $j = 0, 1$ so that

$$\begin{aligned}
h_0'(t) &= \kappa\theta h_1(t) \\
h_0(0) &= 0 \\
h_1'(t) &= b_2 + b_1 h_1(t) \\
h_1(0) &= 0.
\end{aligned}$$

The above can be solved explicitly leading to $h_0(t) = b_2 c_0(t)$ and $h_1(t) = b_2 c_1(t)$ for $c_0(t)$ and $c_1(t)$ derived in equations (11)–(12). Therefore $\mathbb{E}(X(t)) = h_0(t) + h_1(t)v(0)$.

By differentiation of the system (A.1)–(A.4) with respect to w, we obtain the system of ODEs satisfied by $\bar{\Psi}_0(w, u; t)$ and $\bar{\Psi}_1(w, u; t)$

$$
\begin{aligned}
\bar{\Psi}_0'(w,u;t) &= \kappa\theta\bar{\Psi}_1(w,u;t)\\
\bar{\Psi}_0(w,u;0) &= 0\\
\bar{\Psi}_1'(w,u;t) &= \mathrm{i}\eta_1\sigma_1\frac{d^2}{d\bar{u}^2}\varphi_{J_{1,-}}(x)\,\hat{\Psi}_1(w,u;t)\\
&\quad-\left(\eta_1^2\frac{d^2}{d\bar{u}^2}\varphi_{J_{1,-}}(x)+\eta_2^2\frac{d^2}{d\bar{u}^2}\varphi_{J_2}(y)\right)\hat{\Psi}_1(w,u;t)\tilde{\Psi}_1(w,u;t)\\
&\quad+\left(\mathrm{i}\eta_1\frac{d}{d\bar{u}}\varphi_{J_{1,-}}(x)-\mathrm{i}\eta_2\frac{d}{d\bar{u}}\varphi_{J_2}(y)-\kappa\right)\bar{\Psi}_1(w,u;t)\\
\bar{\Psi}_1(w,u;0) &= 0.
\end{aligned}
$$

Setting $u=w=0$, the system reduces to

$$
\begin{aligned}
\bar{\Psi}_0'(0,0;t) &= \kappa\theta\bar{\Psi}_1(0,0;t)\\
\bar{\Psi}_0(0,0;0) &= 0\\
\bar{\Psi}_1'(0,0;t) &= \mathrm{i}\hat{\rho}\hat{\Psi}_1(0,0;t)+\hat{\sigma}_1^2\hat{\Psi}_1(0,0;t)\tilde{\Psi}_1(0,0;t)+b_1\bar{\Psi}_1(0,0;t)\\
\bar{\Psi}_1(0,0;0) &= 0.
\end{aligned}
$$

Let us define $g_1(t)=-\mathrm{i}\hat{\Psi}_1(0,0;t)$, $p_0(t)=-\bar{\Psi}_0(0,0;t)$ and $p_1(t)=-\bar{\Psi}_1(0,0;t)$. The above system then can be rewritten as

$$
\begin{aligned}
p_0'(t) &= \kappa\theta p_1(t)\\
p_0(0) &= 0\\
p_1'(t) &= \hat{\rho}g_1(t)+\hat{\sigma}_1^2 g_1(t)h_1(t)+b_1p_1(t)\\
p_1(0) &= 0.
\end{aligned}
$$

The function $g_1(t)$ follows from the derivation of the expected values of $v(t)$ using a similar argument as for $h_1(t)$, which returns $g_1(t)=e^{b_1t}$. The expression of the covariance follows as the above system can be solved explicitly.

An alternative derivation of the result can be obtained by applying Theorem 6.15 in Eberlein and Kallsen (2019).